

SOA formation and composition from the photo-oxidation of methyl chavicol

K. L. Pereira et al.

# Secondary organic aerosol formation and composition from the photo-oxidation of methyl chavicol (estragole)

K. L. Pereira<sup>1</sup>, J. F. Hamilton<sup>1</sup>, A. R. Rickard<sup>1,2</sup>, W. J. Bloss<sup>3</sup>, M. S. Alam<sup>3</sup>, M. Camredon<sup>4</sup>, A. Muñoz<sup>5</sup>, M. Vásquez<sup>5</sup>, E. Borrás<sup>5</sup>, and M. Ródenas<sup>5</sup>

<sup>1</sup>Wolfson Atmospheric Chemistry Laboratory, Department of Chemistry, University of York, York, UK

<sup>2</sup>National Centre for Atmospheric Science, University of York, York, UK

<sup>3</sup>School of Geography, Earth and Environmental Sciences, University of Birmingham, Birmingham, UK

<sup>4</sup>LISA, UMR CNRS/INSU 7583, University of Paris-Est Créteil, Paris, France

<sup>5</sup>CEAM-UM, EUPHORE, Valencia, Spain

Received: 4 December 2013 – Accepted: 7 December 2013 – Published: 18 December 2013

Correspondence to: J. F. Hamilton (jacqui.hamilton@york.ac.uk)

Published by Copernicus Publications on behalf of the European Geosciences Union.

Title Page

Abstract

Introduction

Conclusions

References

Tables

Figures

⏪

⏩

◀

▶

Back

Close

Full Screen / Esc

Printer-friendly Version

Interactive Discussion

## Abstract

The increasing demand for palm oil for uses in biofuel and food products is leading to rapid expansion of oil palm agriculture. Methyl chavicol (also known as estragole and 1-allyl-4-methoxybenzene) is an oxygenated biogenic volatile organic compound that was recently identified as the main floral emission from an oil palm plantation in Malaysian Borneo. The emissions of methyl chavicol observed may impact regional atmospheric chemistry, but little is known of its ability to form secondary organic aerosol (SOA). The photo-oxidation of methyl chavicol was investigated at the European Photoreactor chamber as a part of the atmospheric chemistry of methyl chavicol (AT-MECH) project. Aerosol samples were collected using a particle into liquid sampler (PILS) and analysed offline using an extensive range of instruments including; high performance liquid chromatography mass spectrometry (HPLC-ITMS), high performance liquid chromatography quadrupole time-of-flight mass spectrometry (HPLC-QTOFMS) and Fourier transform ion cyclotron resonance mass spectrometry (FTICR-MS). The SOA yield was determined as 18–29% depending on initial precursor (VOC:NO<sub>x</sub>) mixing ratios. In total, 59 SOA compounds were observed and the structures of 10 compounds have been identified using high resolution tandem mass spectrometry. The addition of hydroxyl and/or nitro functional groups to the aromatic ring appears to be an important mechanistic pathway for aerosol formation. This results in the formation of compounds with both low volatility and high O:C ratios, where functionalisation rather than fragmentation is mainly observed as a result of the stability of the ring. The SOA species observed can be characterized as semi-volatile to low volatile oxygenated organic aerosol (SVOOA and LVOOA) components and therefore may be important in aerosol formation and growth.

## SOA formation and composition from the photo-oxidation of methyl chavicol

K. L. Pereira et al.

Title Page

Abstract

Introduction

Conclusions

References

Tables

Figures



Back

Close

Full Screen / Esc

Printer-friendly Version

Interactive Discussion



## 1 Introduction

The atmospheric oxidation of volatile organic compounds (VOCs) in the presence of  $\text{NO}_x$  results in the formation of tropospheric ozone and secondary organic aerosol (SOA). Whilst SOA formation is known to have adverse effects on climate and human health (Solomon et al., 2007; Bernstein et al., 2004; Davidson et al., 2005; Pöschl, 2005), the VOC oxidation pathways leading to SOA formation are poorly understood (Hallquist et al., 2009). It has been estimated that as many as  $10^4$ – $10^5$  VOCs have been detected in the atmosphere, all of which may undergo atmospheric oxidation and contribute to SOA formation (Goldstein and Galbally, 2007). Approximately 90 % of all global VOC emissions are from biogenic sources (Guenther et al., 1995). The most abundant biogenic emissions are attributed to isoprene (35–40 %), monoterpenes (11–25 %) and oxygenated VOCs (reactive other VOCs and other VOCs, 20–30 %) (Guenther et al., 1995, 2000). The largest source of biogenic VOC emissions are from vegetation; including trees (which account for  $\sim 71$  % of emissions; Guenther et al., 1995), shrubs and crops, with a small emission source from grasslands and soils (Guenther et al., 1995, 2000; Zimmerman, 1979; Wiedinmyer et al., 2004). Oxygenated VOCs (OVOCs) have received more attention recently due to the advances in instrumentation to detect and quantify these compounds in the ambient atmosphere. Despite this, significant uncertainties still remain in our knowledge of the sources, chemical composition and atmospheric oxidation mechanisms of OVOCs, in particular higher molecular weight species ( $> C_5$ ) (Singh et al., 2000; Steiner et al., 2008; Taipale et al., 2012; Schade and Goldstein, 2001; Bouvier-Brown, 2008).

Methyl chavicol ( $\text{C}_{10}\text{H}_{12}\text{O}$ ), also known as estragole and 1-allyl-4-methoxybenzene, is a  $\text{C}_{10}$  aromatic biogenic OVOC emitted from a variety of pine trees (including ponderosa pine), shrubs (*Clausena dunniana*, straggley Baeckea) and common herbs (basil, fennel, tarragon) (Werker et al., 1994; Simon et al., 1990; Southwell et al., 2003; Mirov, 1961; Bouvier-Brown et al., 2009; De Vincenzi et al., 2000; Barazani et al., 2002; Adams, 2007; Holzinger et al., 2005, 2010). A recent publication identified significant

ACPD

13, 33105–33144, 2013

### SOA formation and composition from the photo-oxidation of methyl chavicol

K. L. Pereira et al.

Title Page

Abstract

Introduction

Conclusions

References

Tables

Figures



Back

Close

Full Screen / Esc

Printer-friendly Version

Interactive Discussion



**SOA formation and composition from the photo-oxidation of methyl chavicol**

K. L. Pereira et al.

Title Page

Abstract

Introduction

Conclusions

References

Tables

Figures

⏪

⏩

◀

▶

Back

Close

Full Screen / Esc

Printer-friendly Version

Interactive Discussion

methyl chavicol emissions above the canopy of an oil palm plantation in Malaysian Borneo, with a mean midday flux of  $0.81 \text{ mg m}^{-2} \text{ h}^{-1}$  and a mean mixing ratio of 3.0 ppbv (maximum mixing ratio observed  $\sim 7.0$  ppbv) (Misztal et al., 2010). Methyl chavicol emissions from palm oil plantations were estimated to result in a global emission of  $\sim 0.5 \text{ Tgyr}^{-1}$  (Misztal et al., 2010). There are currently 43 oil palm producing countries, with the majority of oil palm plantations concentrated in Indonesia and Malaysia (FAO-STAT, 2012). In 2011, there were approximately 7.7 million hectares (Mha) of oil palm plantations in Indonesia (USDA, 2013) and 5.0 Mha in Malaysia (MPOB, 2012). The increasing demand for palm oil for uses in food products and biofuels is resulting in the rapid expansion of oil palm agriculture (Fitzherbert et al., 2008). Consequently, methyl chavicol emissions are likely to have a considerable effect on regional chemistry in locations where oil palm plantations are significant. Despite this, there have been few literature reports which have investigated the atmospheric fate of methyl chavicol, including gas-phase degradation, SOA formation, composition and yields.

The gas phase products formed from the oxidation of methyl chavicol with hydroxyl radicals ( $\bullet\text{OH}$ ), and ozone ( $\text{O}_3$ ) has been investigated by Lee et al. (2006a) and Lee et al. (2006b), and more recently by Bloss et al. (2012), who reported measurements of the gas-phase reactivity of methyl chavicol with  $\bullet\text{OH}$  and  $\text{O}_3$ , and by Gai et al. (2013) who in addition investigated the oxidation of methyl chavicol with  $\text{NO}_3$ . In the study performed by Lee et al. (2006b) the photo-oxidation of methyl chavicol resulted in significant SOA formation (yield 40%) and the formation of two abundant structurally unidentified gas phase compounds, MW 136 ( $\text{C}_8\text{H}_8\text{O}_2$ , yield  $42 \pm 9\%$ ) and MW 150 ( $\text{C}_9\text{H}_{10}\text{O}_2$ , yield  $23 \pm 5\%$ ), detected using proton transfer reaction mass spectrometry (PTR-MS). Bouvier-Brown et al. (2009) identified MW 136 as 4-methoxybenzaldehyde in the aerosol phase at Blodgett forest (California, US) and suggested the identification of pinonaldehyde (MW 150) (Holzinger et al., 2005) could be in part attributed to 4-methoxybenzene acetaldehyde (MW 150) identified in Lee et al. (2006b). In addition, Cahill et al. (2006) tentatively identified 4-methoxybenzene acetaldehyde in aerosol samples collected in the Sierra Nevada Mountains. More recently, Gai et al. (2013)



performed during May 2012 and the initial mixing ratios, chamber temperatures and relative humidities are presented in Table 1.

The chamber was cleaned before each experiment by flushing with scrubbed dry air overnight. Methyl chavicol was introduced into the chamber through a heated air stream. An extensive range of monitors were used to measure chamber temperature (temperature sensor, model PT100), pressure (Barometer, model AIR-DB-VOC), humidity (Hygrometer Watz, model Walz-TS2), solar intensity ( $J_{\text{NO}_2}$  Filter Radiometer), ozone (Monitor Labs, model 9810) and  $\text{NO}_x$  (Teledyne API, model  $\text{NO}_x\text{-API-T200UP}$ ; photolytic converter). PTR-MS (Ionikon Analytik) and Fourier transform infra red (FTIR Nicolet Magna, model 550), coupled to a white-type mirror system with an optical path length of 326.8 m, were used to monitor methyl chavicol decay and product formation. The chamber dilution rate was calculated by measuring the decay of an inert tracer gas, sulphur hexafluoride ( $\text{SF}_6$ ), using FTIR; typical pseudo-first-order rate constants of  $2 \times 10^{-5} \text{ s}^{-1}$  were obtained, corresponding to a dilution lifetime around 14 h. The formation and evolution of secondary organic aerosol (SOA) was measured using a scanning mobility particle sizer (TSI Incorporated, model 3080) consisting of a differential mobility analyzer (model 3081) and a condensation particle counter (model 3775).

## 2.2 Aerosol sampling and sample preparation

A Brechtel Manufacturing Inc (California, US) model 4002 PILS was used for aerosol collection. The PILS inlet was connected to the chamber outlet using approximately 1.5 m of 1/4" stainless steel tubing. Aerosol samples were collected using a  $\text{PM}_{10}$  impactor, with an average flow rate of  $13 \text{ L min}^{-1}$ . Acidic, basic and organic gases were removed from the sampled air through the use of denuders, prepared as per manufacture instructions. The wash flow rate was set at  $240 \mu\text{L min}^{-1}$  and consisted of optima LC-MS grade water (Fisher Scientific, UK). The sample flow rate transferred the aerosol water mixture (optima LC-MS grade water) into sealed vials at a flow rate of  $200 \mu\text{L min}^{-1}$  for 30 min per sample. Samples were collected before the addition of

### SOA formation and composition from the photo-oxidation of methyl chavicol

K. L. Pereira et al.

Title Page

Abstract

Introduction

Conclusions

References

Tables

Figures

⏪

⏩

◀

▶

Back

Close

Full Screen / Esc

Printer-friendly Version

Interactive Discussion

methyl chavicol or NO into the chamber and continued sampling until after the chamber was closed. After sample collection, punctured vial caps were replaced and securely sealed with parafilm. All vials were wrapped in foil to minimise potential degradation from photolysis and were stored at  $-20^{\circ}\text{C}$  until analysis. Collected PILS samples were evaporated to dryness using a V10 vacuum solvent evaporator (Biotage, USA) and redissolved in 300  $\mu\text{L}$  of 50 : 50 methanol : water (optima LC-MS grade, Fisher, UK), with the exception of experiment  $\text{MC}_{\text{high}}$ , which was redissolved in 500  $\mu\text{L}$ .

## 2.3 HPLC-ITMS

SOA composition was investigated using an Agilent 1100 series high performance liquid chromatography (HPLC, Berkshire, UK) coupled to a HTC Plus ion trap mass spectrometer (IT-MS, Bruker Daltonics, Bremen, Germany). A reversed phase Pinnacle C18 150 mm  $\times$  4.6 mm, 5  $\mu\text{m}$  particle size column (Thames Resteck, UK) was used. The HPLC mobile phase composition consisted of (A) water (optima LC-MS grade, Fisher, UK) with 0.1 % formic acid (Sigma Aldrich, UK) and (B) methanol (optima LC-MS grade, Fisher, UK). Gradient elution was used, starting at 90 % (A) 10 % (B), moving to 0 % (A) 100 % (B) over 60 min, returning to the initial starting conditions at 65 min. A 5 min pre-run consisting of the starting mobile phase composition was performed before each sample injection. The flow rate was set at 0.6  $\text{mL min}^{-1}$  with a sample injection volume of 60  $\mu\text{L}$ . Electrospray ionisation (ESI) was used, with a dry gas flow rate of 12  $\text{L min}^{-1}$ , a dry gas temperature of 365  $^{\circ}\text{C}$  and nebuliser gas pressure of 70 psi (oxygen free nitrogen, OFN, BOC, UK). The MS was operated in alternating polarity mode, scanning from  $m/z$  50 to 600. Tandem MS was achieved through the automated  $\text{MS}^2$  function within the Esquire software (Bruker Daltonics, software version 5.2).

## 2.4 FTICR-MS

A solariX Fourier transform ion cyclotron resonance mass spectrometer with a 9.4 T superconducting magnet (Bruker Daltonics, Coventry, UK) was used and externally

ACPD

13, 33105–33144, 2013

## SOA formation and composition from the photo-oxidation of methyl chavicol

K. L. Pereira et al.

Title Page

Abstract

Introduction

Conclusions

References

Tables

Figures

⏪

⏩

⏴

⏵

Back

Close

Full Screen / Esc

Printer-friendly Version

Interactive Discussion



**SOA formation and composition from the photo-oxidation of methyl chavicol**

K. L. Pereira et al.

Title Page

Abstract

Introduction

Conclusions

References

Tables

Figures

⏪

⏩

◀

▶

Back

Close

Full Screen / Esc

Printer-friendly Version

Interactive Discussion

calibrated using L-Arginine (Sigma Aldrich, UK, purity 98 %). Samples were introduced into the ESI source through direct infusion, using a Hamilton 50  $\mu\text{L}$  syringe (Hamilton, Switzerland) at a flow rate of 120  $\mu\text{L min}^{-1}$ . Spectra were acquired in both positive and negative ionisation modes over a scan range of  $m/z$  50–800. The ESI parameters were set to a dry gas flow rate of 3.7  $\text{L min}^{-1}$ , dry gas temperature of 220  $^{\circ}\text{C}$ , and a nebulizer gas pressure of 1.2 bar (nitrogen, BOC, UK). Broadband detection mode was used, with 64 spectra averages obtained for each spectrum. Ion accumulation in the ICR cell was set to 0.5 s with a source accumulation time of 0.002 s. The collision RF and ion cooler time was set to favour lower masses at 1300 Vpp and 0.010 s, respectively. An approximate resolution of 38 000 at  $m/z$  400 was obtained for both ionisation modes. The spectral analysis was performed using DataAnalysis 4.0 software (Bruker Daltonics, Bremen, Germany). Monoisotopic elemental formulae were calculated using the following restrictions; unlimited C, H and O were allowed and up to 3 N atoms, O : C < 3, H : C > 0.5, DBE < 20, and in positive mode, Na and K adducts were also allowed. The accuracy of the molecular formulae (elemental composition) assignment is shown by the error; where the error equals the difference between the exact and measured mass for the assigned molecular formula. The mass error (also referred to as mass accuracy) is displayed in ppm and is calculated by dividing the mass error by the exact mass for the assigned molecular formula and multiplying by  $10^6$ . The molecular formula score refers to the fit of the theoretical and measured isotopic distribution and abundance for the assigned molecular formula, and is displayed in percentage. The molecular formula score is not calculated for a signal to noise ( $S/N$ ) ratio below 5. The combination of a high score and low mass accuracy will result in few potential molecular formula assignments for a compound at a given  $m/z$ . A compound with an  $m/z$  below 300, with a high score (100 %) and low mass accuracy (< 5 ppm) results in only one potential molecular formula (Kind and Fiehn, 2006).





respectively, showing a larger yield at higher initial mixing ratios as seen previously (Song et al., 2005).

### 3.1 SOA composition

The PILS samples were analysed using a series of complementary analytical techniques. Initially, the HPLC-ITMS was used to screen the PILS samples for SOA species. Any compounds observed in the PILS samples before the introduction of methyl chavicol and NO into the chamber in  $MC_{high}$  and  $MC_{low}$  were excluded from further analysis. Compounds which displayed changes in their chromatographic peak areas (and thus concentration) were investigated further. In the  $MC_{high}$  experiment, 59 SOA compounds were observed in the PILS samples using HPLC-ITMS. Of these compounds, 57 were observed with matching retention times and/or fragmentation patterns in the  $MC_{low}$  experiment. In  $MC_{high}$ , fragmentation data was obtained for 56 of the 59 SOA compounds using HPLC-ITMS<sup>2</sup>. In many cases it was not possible to identify the compound structures of the SOA species due to the low mass resolution of the ITMS and lack of commercially available standards. This resulted in the use of the FTICR-MS to aid in the identification of the SOA molecular formulae and compound structures. The use of FTICR-MS significantly aided in compound identification, providing the molecular formulae for 49 of the 59 SOA compounds with average error of 0.14 ppm for negative ionisation mode and 5.72 ppm for positive ionisation mode. FTICR-MS<sup>2</sup> could not be performed due to the lack of prior chromatographic separation and the low concentration of the SOA compounds. Instead, HPLC-QTOFMS<sup>2</sup> was used to obtain high mass resolution compound fragmentation data for the SOA compounds. The HPLC-QTOFMS identified the molecular formulae of 54 of the 59 SOA compounds with an average error of 4.52 ppm for negative ionisation mode and 27.29 ppm for positive ionisation mode. The use of the HPLC-QTOFMS was complementary to the FTICR-MS, allowing the comparison of two high mass resolution data sets to determine the molecular formulae of the SOA compounds, as shown in Table 2 and Supplement Tables 1

## SOA formation and composition from the photo-oxidation of methyl chavicol

K. L. Pereira et al.

Title Page

Abstract

Introduction

Conclusions

References

Tables

Figures

⏪

⏩

◀

▶

Back

Close

Full Screen / Esc

Printer-friendly Version

Interactive Discussion





**SOA formation and composition from the photo-oxidation of methyl chavicol**

K. L. Pereira et al.

Title Page

Abstract

Introduction

Conclusions

References

Tables

Figures

⏪

⏩

◀

▶

Back

Close

Full Screen / Esc

Printer-friendly Version

Interactive Discussion

is due to the loss of water ( $\text{H}_2\text{O}$ ) occurring through hydrogen abstraction, Fig. 2a. The base peak loss of  $\text{H}_2\text{O}$  would suggest the presence of an aliphatic alcohol, most likely terminal. The loss of  $\text{H}_2\text{O}$  results in an intermolecular rearrangement of the fragment ion, resulting in the formation of a double bond, indicated by the increase in the DBE by 1. The fragment ion at  $m/z$  182 has formed as a result of a subsequent loss of  $\text{C}_2\text{H}_2\text{O}$  from  $m/z$  224, which is supported by the decrease in the DBE by 1 for the remaining fragment ion. The fragment ion at  $m/z$  182 results from a total loss of  $\text{C}_2\text{H}_4\text{O}_2$ , suggesting the presence of a second hydroxyl group on the leaving group, most likely on the adjacent carbon to the first alcohol group, Fig. 2b. The fragment ion at  $m/z$  167 has formed as a result of an odd electron cleavage (OE), resulting in the formation of  $[\text{C}_7\text{H}_5\text{NO}_4]^{*-}$  and the loss of  $[\text{C}_3\text{H}_7\text{O}_2]^\bullet$ , Fig. 2c. OE cleavages are unusual in CID and are often associated with resonance stabilised ring structures and nitrogen containing functional groups (Fu et al., 2006; Holčápek et al., 2007, 2010; Hayen et al., 2002).

Assuming the remaining deprotonated radical fragment ion at  $m/z$  167  $[\text{C}_7\text{H}_5\text{NO}_4]^{*-}$  is a substituted methoxyphenyl, the subtraction of the methoxy  $[\text{OCH}_3]$  and aromatic  $[\text{C}_6\text{H}_2]^-$  group from the molecular formula would leave  $\text{N}_1\text{O}_3$  unaccounted for. This suggests either a nitrate group ( $\text{R-ONO}_2$ ), or a hydroxyl ( $\text{R-OH}$ ) and a nitro ( $\text{R-NO}_2$ ) group are attached to the ring. The presence of a nitrate group on the ring is likely to result in the loss of  $\text{NO}_2$  or  $\text{ONO}_2$  from the fragmentation of the carbon-oxygen or oxygen-nitrogen bond during CID (Zhao and Yinon, 2002; Holčápek et al., 2010). Furthermore, the lability of the nitrate group often results in spontaneous fragmentation in the softest ESI conditions, resulting in the fragment ions  $\text{ONO}_2$  and  $\text{NO}_2$  at  $m/z$  63 and  $m/z$  47, respectively (Holčápek et al., 2010; Yinon et al., 1997). However, no fragment ion at  $m/z$  63 for  $\text{ONO}_2$  was observed. A peak at  $m/z$  137 (intensity 1.33 %) was observed and was attributed to  $[\text{C}_7\text{H}_5\text{O}_3]^{*-}$ , the loss of  $\text{NO}$  from the fragment ion at  $m/z$  167  $[\text{C}_7\text{H}_5\text{NO}_4]^{*-}$ , Fig. 2c. The loss of  $\text{NO}$  is a typical for nitro functional groups in negative ionisation mode using CID (Holčápek et al., 2010; Fu et al., 2006; Schmidt et al., 2006; Yinon et al., 1997). The rearrangement of bonds from  $\text{R-NO}_2$  to  $\text{R-ONO}$  results in the loss of  $\text{NO}$  (Schmidt et al., 2006). Nitro functional groups usually result





**SOA formation and composition from the photo-oxidation of methyl chavicol**

K. L. Pereira et al.

Title Page

Abstract

Introduction

Conclusions

References

Tables

Figures

⏪

⏩

◀

▶

Back

Close

Full Screen / Esc

Printer-friendly Version

Interactive Discussion

(Atkinson, 2000, 1997b; Cvetanovic, 1976). The resulting  $\beta$ -hydroxyalkyl radicals react predominantly with  $O_2$  to form  $\beta$ -hydroxyperoxy radicals. The high concentration of NO at the beginning of  $MC_{high}$  and  $MC_{low}$  will result in the conversion of NO to  $NO_2$  (leading to  $O_3$  formation) and the formation of  $\beta$ -hydroxyalkoxy radicals as the major pathway.

$\beta$ -hydroxyalkoxy radicals can react with  $O_2$ , decompose or isomerize. Decomposition and isomerisation are expected to be the dominant pathways, with the exception of the  $HOCH_2CH_2O^*$  radical (from ethene +  $^*OH$ ), for which decomposition and reaction with  $O_2$  can be competitive (Atkinson, 1997b, a; Fuchs et al., 2011).

For both types of  $\beta$ -hydroxyalkoxy radicals formed, decomposition followed by rapid reaction with  $O_2$  leads to the formation of formaldehyde,  $HO_2$  and (4-methoxyphenyl)acetaldehyde (Atkinson, 1997b; Orlando et al., 2003). Isomerisation through a 1, 5-H atom shift from the aromatic ring to the HC chain is suggested to be of minor importance due to the resonance stability of the ring. The reaction with  $O_2$  (minor pathway) would result in the loss of  $HO_2$  and the formation of the observed first generation compound, 1-hydroxy-3-(4-methoxyphenyl)propan-2-one (compound 9), Fig. 4a. Further oxidation of this compound through the addition of a hydroxyl radical to the ring results in the formation of 1-hydroxy-3-(3-hydroxy-4-methoxyphenyl)propan-2-one (compound 10), Fig. 4b. As discussed in the previous section, the initial hydroxyl addition to the ring will occur at the ortho position to the methoxy group, the position which is most energetically favoured and resonance stabilised. Compound 8, 2-hydroxy-3-(3-hydroxy-4-methoxyphenyl)propanal, is also suggested to be a second generation compound which has formed through the oxidation of the primary  $\beta$ -hydroxyalkoxy radicals with  $O_2$  (the less favoured pathway) and has been further oxidised by the addition of a hydroxyl radical to the ring, Fig. 4c.

As a relatively “low  $NO_x$  state” is entered in  $MC_{high}$  and  $MC_{low}$  the  $RO_2 + RO_2$  reaction will begin to dominate over the competing reaction with NO (Atkinson, 1997b; Stockwell et al., 1990). The cross/self reaction of  $\beta$ -hydroxyperoxy radicals will proceed mainly through two pathways; the radical pathway and non-radical pathway (hydrogen abstraction), with the radical pathway accounting for approximately 30–80 % of

**SOA formation and composition from the photo-oxidation of methyl chavicol**

K. L. Pereira et al.

Title Page

Abstract

Introduction

Conclusions

References

Tables

Figures

⏪

⏩

◀

▶

Back

Close

Full Screen / Esc

Printer-friendly Version

Interactive Discussion

the  $\text{RO}_2 + \text{RO}_2$  reaction (Atkinson, 1997b; Madronich and Calvert, 1990). The radical pathway (major pathway) will result in the formation of  $\beta$ -hydroxyalkoxy radicals with the loss of  $\text{O}_2$ . The  $\beta$ -hydroxyalkoxy radicals can then undergo oxidation through the same mechanisms as discussed above, resulting in a secondary pathway for the formation of compounds 8, 9 and 10, Fig. 4d–f, respectively. A third minor pathway to the formation of compounds 8, 9 and 10 can also occur through the  $\text{RO}_2 + \text{RO}_2$  non radical pathway; where one peroxy radical abstracts a hydrogen atom from another peroxy radical, resulting in the formation of an alcohol and carbonyl, respectively, with the loss of  $\text{O}_2$  (Madronich and Calvert, 1990; Howard and Ingold, 1968). The hydrogen atom is abstracted from the carbon bonded to the peroxy radical, thus the abstraction of a hydrogen atom from a secondary  $\beta$ -hydroxyperoxy radical will result in the formation of 1-hydroxy-3-(4-methoxyphenyl)propan-2-one (compound 9), Fig. 4g. The further oxidation of this compound through the reaction with  $\cdot\text{OH}$  will result in the formation of 1-hydroxy-3-(3-hydroxy-4-methoxyphenyl)propan-2-one (compound 10), Fig. 4h. Moreover, the abstraction of a hydrogen from a primary  $\beta$ -hydroxyperoxy radical followed by the further oxidation of an  $\cdot\text{OH}$  radical to the ring, will result in the formation of 2-hydroxy-3-(3-hydroxy-4-methoxyphenyl)propanal (compound 8), Fig. 4i.

The formation of the diol on the HC chain of compound 1 [3-(5-hydroxy-4-methoxy-2-nitrophenyl)propane-1,2-diol], and compound 5 [3-(3-hydroxy-4-methoxyphenyl)propane-1,2-diol], could have occurred through two mechanisms; unimolecular isomerisation of the  $\beta$ -hydroxyalkoxy radical through a 1,5 H-atom shift, or the self/cross  $\text{RO}_2$  reactions of the  $\beta$ -hydroxyperoxy radicals through the non-radical pathway. The isomerisation pathway would seem unlikely due to the formation of a alkyl radical on the carbon where the H-atom was abstracted, which could decompose, isomerise, or react with  $\text{O}_2$ , with the latter resulting in the formation of a more oxidised product than observed. Decomposition would result in the formation of a compound with fewer carbon atoms than required, and isomerisation would still result in an alkyl radical. The self/cross reactions of  $\beta$ -hydroxyperoxy radicals would appear to be the more likely pathway, particularly under low  $\text{NO}_x$  conditions. After



**SOA formation and composition from the photo-oxidation of methyl chavicol**

K. L. Pereira et al.

Title Page

Abstract

Introduction

Conclusions

References

Tables

Figures

⏪

⏩

◀

▶

Back

Close

Full Screen / Esc

Printer-friendly Version

Interactive Discussion

between the two studies. Lee et al. (2006b) used ammonium sulfate seed (compared to the nucleation only experiments presented here), which has been shown to substantially increase SOA yields (Czoschke et al., 2003; Gao et al., 2004; Jang et al., 2002; Zhou et al., 2011). In addition, the percentage relative humidity (% RH) was approximately 5 times greater in the study performed by Lee et al. (2006b). Recent publications have shown that the SOA mass formed from a substituted aromatic compound (*p*-xylene), increases with increasing % RH, approximately by a factor of 2 over a % RH range of 5 to 75 % (Zhou et al., 2011; Healy et al., 2009). Moreover, the hydrocarbon to NO<sub>x</sub> ratio (HC : NO<sub>x</sub>) in the study performed by Lee et al. (2006b) was greater (HC/NO<sub>x</sub> = ~ 8) than that in this study (HC/NO<sub>x</sub> = ~ 5), which may account for the lower SOA yield obtained in this study (Kroll and Seinfeld, 2008). Nevertheless, it is clear the photo-oxidation of methyl chavicol results in significant SOA formation. Recent literature has shown oxygenated biogenic VOCs containing 10 carbon atoms (including eucalyptol, verbenone, linalool) resulted in an SOA yield between 16 to 20 %, with the use of acidic seed (Linuma et al., 2008; Varutbangkul et al., 2006; Lee et al., 2006b). It is difficult to directly compare SOA yields from the oxidation of a similar VOC precursor in the literature due to the limitations of using chamber derived data (Camredon et al., 2007). However, reported SOA yields of methyl chavicol were the highest of all oxygenated VOCs investigated (SOA yield 26–40 %) (Lee et al., 2006b; Varutbangkul et al., 2006). Although these experiments are at concentrations higher than the real atmosphere, they suggest that methyl chavicol can act as an important SOA precursor in regions where methyl chavicol emissions are significant, such as downwind from pine forests and oil palm plantations.

Four compounds with a MW of 122, 136, 150 and 166 were observed in the gas phase using PTR-MS and may be attributed to 4-methoxytoluene, 4-methoxybenzaldehyde, 4-methoxybenzene acetaldehyde and (4-methoxyphenyl)acetic acid, respectively, in agreement with Lee et al. (2006b), Spada et al. (2008) and Gai et al. (2013). However, in contrast to Cahill et al. (2006) and Bouvier-Brown et al. (2009) 4-methoxybenzaldehyde (MW 136) and 4-methoxybenzene acetaldehyde

**SOA formation and composition from the photo-oxidation of methyl chavicol**

K. L. Pereira et al.

Title Page

Abstract

Introduction

Conclusions

References

Tables

Figures

⏪

⏩

◀

▶

Back

Close

Full Screen / Esc

Printer-friendly Version

Interactive Discussion

(MW 150) were not identified in the aerosol phase in this study. Compound vapour pressures were calculated using the UManSysProp website (<http://ratty.cas.manchester.ac.uk/informatics/>) at 298.15 K, using the Nannoolal vapour pressure and boiling point extrapolation method (Nannoolal et al., 2004, 2008) and the saturation concentration ( $C^*$ ,  $\mu\text{g m}^{-3}$ ) determined (Donahue et al., 2006a). The calculated volatility of these compounds suggests they are intermediate VOCs (4-methoxybenzaldehyde,  $C^* = 4.96 \times 10^5 \mu\text{g m}^{-3}$  and 4-methoxybenzene acetaldehyde,  $C^* = 3.02 \times 10^5 \mu\text{g m}^{-3}$ ). The use of gas phase scrubbers for organics in the PILS sampler used in this study may indicate that previous ambient observations are due to positive artifacts from gas phase absorption to filters.

The saturation concentration ( $C^*$ ,  $\mu\text{g m}^{-3}$ ) (Donahue et al., 2006a) and O : C ratio were determined for all the identified compounds and plotted in a O : C /  $\log_{10}(C^*$ ,  $\mu\text{g m}^{-3})$  volatility basis set space (Donahue et al., 2013; Jimenez et al., 2009), as shown in Fig. 5. All of the identified SOA compounds retained the aromatic ring, with O : C ratios between 0.30 to 0.63 and H : C ratios between 1.11 and 1.40. The oxidation of methyl chavicol and its early generation products resulted in the formation of low vapour pressure and a high O : C ratio species, due to the lack of ring fragmentation. This resulted in the movement of the SOA compounds to lower volatilities and higher O : C ratios, thus functionalisation rather than fragmentation was mainly observed. The majority of the SOA species underwent oxidation on the aromatic ring, through the addition of  $\cdot\text{OH}$  and/or  $\text{NO}_2$ . The formation of compound 1 (3-(5-hydroxy-4-methoxy-2-nitrophenyl)propane-1,2-diol) through the addition of a  $\text{NO}_2$  group on the aromatic ring resulted in the movement of this species to the low volatility oxygenated organic aerosol region (LVOOA), and just outside the extremely low volatility oxygenated organic aerosol (ELVOOA) nucleator region proposed by Donahue et al. (2013). Ring addition appears to be an important pathway, resulting in the formation of low volatility species with high O : C ratios, which may also be important for other aromatic compounds. The structures of only 10 of the 59 SOA compounds have so far been iden-

tified. Further work is required to characterize the SOA formed from methyl chavicol oxidation at different mixing ratios and with different oxidants (O<sub>3</sub>, NO<sub>3</sub>).

**Supplementary material related to this article is available online at**  
**[http://www.atmos-chem-phys-discuss.net/13/33105/2013/  
acpd-13-33105-2013-supplement.pdf](http://www.atmos-chem-phys-discuss.net/13/33105/2013/acpd-13-33105-2013-supplement.pdf)**

*Acknowledgements.* The assistance of scientists at EUPHORE and the York Centre of Excellence in Mass Spectrometry is gratefully acknowledged. This work was supported by EUROCHAMP-2 (TA Project E2-2011-04-19-0059). ARR acknowledges the support of the National Centre for Atmospheric Science. The York Centre of Excellence in Mass Spectrometry was created thanks to a major capital investment through Science City York, supported by Yorkshire Forward with funds from the Northern Way Initiative. KEP acknowledges support of a NERC PhD studentship (NE106026057).

## References

- Adams, R. P.: Identification of Essential Oil Components by Gas Chromatography/Mass Spectrometry, 4th edn., Allured Publishing Corporation, Carol Stream, 2007.
- Atkinson, R.: Gas-phase tropospheric chemistry of organic compounds, J. Phys. Chem. Ref. Data, Monograph, 2, 1–216, 1994.
- Atkinson, R.: Atmospheric reactions of alkoxy and  $\beta$ -hydroxyalkoxy radicals, Int. J. Chem. Kinet., 29, 99–111, doi:10.1002/(sici)1097-4601(1997)29:2<99::aid-kin3>3.0.co;2-f, 1997a.
- Atkinson, R.: Gas-phase tropospheric chemistry of volatile organic compounds: 1. Alkanes and alkenes, J. Phys. Chem. Ref. Data, 26, 215–290, 1997b.
- Atkinson, R.: Atmospheric chemistry of VOCs and NO<sub>x</sub>, Atmos. Environ., 34, 2063–2101, doi:10.1016/s1352-2310(99)00460-4, 2000.
- Barazani, O., Cohen, Y., Fait, A., Diminshtein, S., Dudai, N., Ravid, U., Putievsky, E., and Friedman, J.: Chemotypic differentiation in indigenous populations of *Foeniculum vulgare* var. *vulgare* in Israel, Biochem. Syst. Ecol., 30, 721–731, 2002.

## SOA formation and composition from the photo-oxidation of methyl chavicol

K. L. Pereira et al.

Title Page

Abstract

Introduction

Conclusions

References

Tables

Figures

⏪

⏩

◀

▶

Back

Close

Full Screen / Esc

Printer-friendly Version

Interactive Discussion



**SOA formation and composition from the photo-oxidation of methyl chavicol**

K. L. Pereira et al.

Title Page

Abstract

Introduction

Conclusions

References

Tables

Figures

⏪

⏩

◀

▶

Back

Close

Full Screen / Esc

Printer-friendly Version

Interactive Discussion

- Becker, K.: EUPHORE: Final Report to the European Commission, Contract# EV5V-CT92-0059, Bergische Universität Wuppertal, Wuppertal, Germany, 1996.
- Bernstein, J. A., Alexis, N., Barnes, C., Bernstein, I. L., Nel, A., Peden, D., Diaz-Sanchez, D., Tarlo, S. M., and Williams, P. B.: Health effects of air pollution, *J. Allergy Clin. Immun.*, 114, 1116–1123, 2004.
- Bloss, C., Wagner, V., Bonzanini, A., Jenkin, M. E., Wirtz, K., Martin-Reviejo, M., and Pilling, M. J.: Evaluation of detailed aromatic mechanisms (MCMv3 and MCMv3.1) against environmental chamber data, *Atmos. Chem. Phys.*, 5, 623–639, doi:10.5194/acp-5-623-2005, 2005.
- Bloss, W. J., Alam, M. S., Rickard, A. R., Hamilton, J. F., Pereira, K. L., Camredon, M., Muñoz, A., Vázquez, M., Alacreu, P., Ródenas, M., and Vera, T.: Atmospheric chemistry of methyl chavicol (estragole), AGU Fall Meeting, San Francisco, Fall meeting 3 to 7 December 2012, A33L-0313, 2012.
- Bouvier-Brown, N. C.: Quantifying Reactive Biogenic Volatile Organic Compounds: Implications for Gas- and Particle-Phase Atmospheric Chemistry, ProQuest, University of California, Berkeley, CA, 2008.
- Bouvier-Brown, N. C., Goldstein, A. H., Worton, D. R., Matross, D. M., Gilman, J. B., Kuster, W. C., Welsh-Bon, D., Warneke, C., de Gouw, J. A., Cahill, T. M., and Holzinger, R.: Methyl chavicol: characterization of its biogenic emission rate, abundance, and oxidation products in the atmosphere, *Atmos. Chem. Phys.*, 9, 2061–2074, doi:10.5194/acp-9-2061-2009, 2009.
- Bursey, M. M.: Influence of steric inhibition of resonance on ion intensities in mass spectra, *J. Am. Chem. Soc.*, 91, 1861–1862, doi:10.1021/ja01035a053, 1969.
- Bursey, M. M. and McLafferty, F. W.: Rearrangements and “flat-topped metastable ions” in the mass spectra of substituted nitrobenzenes, *J. Am. Chem. Soc.*, 88, 5023–5025, doi:10.1021/ja00973a047, 1966.
- Cahill, T. M., Seaman, V. Y., Charles, M. J., Holzinger, R., and Goldstein, A. H.: Secondary organic aerosols formed from oxidation of biogenic volatile organic compounds in the Sierra Nevada Mountains of California, *J. Geophys. Res.*, 111, D16312, doi:10.1029/2006JD007178, 2006.
- Calvert, J. G., Atkinson, R., Kerr, J., Madronich, S., Moortgat, G., Wallington, T. J., and Yarwood, G.: *The Mechanisms of Atmospheric Oxidation of the Alkenes*, Oxford University Press, New York, 2000.



**SOA formation and composition from the photo-oxidation of methyl chavicol**

K. L. Pereira et al.

Title Page

Abstract

Introduction

Conclusions

References

Tables

Figures

⏪

⏩

◀

▶

Back

Close

Full Screen / Esc

Printer-friendly Version

Interactive Discussion

- Fu, X., Zhang, Y., Shi, S., Gao, F., Wen, D., Li, W., Liao, Y., and Liu, H.: Fragmentation study of hexanitrostilbene by ion trap multiple mass spectrometry and analysis by liquid chromatography/mass spectrometry, *Rapid Commun. Mass Sp.*, 20, 2906–2914, 2006.
- Fuchs, H., Bohn, B., Hofzumahaus, A., Holland, F., Lu, K. D., Nehr, S., Rohrer, F., and Wahner, A.: Detection of HO<sub>2</sub> by laser-induced fluorescence: calibration and interferences from RO<sub>2</sub> radicals, *Atmos. Meas. Tech.*, 4, 1209–1225, doi:10.5194/amt-4-1209-2011, 2011.
- Gai, Y., Wang, W., Ge, M., Kjaergaard, H. G., Jørgensen, S., and Du, L.: Methyl chavicol reactions with ozone, OH and NO<sub>3</sub> radicals: rate constants and gas-phase products, *Atmos. Environ.*, 77, 696–702, doi:10.1016/j.atmosenv.2013.05.041, 2013.
- Gao, S., Ng, N. L., Keywood, M., Varutbangkul, V., Bahreini, R., Nenes, A., He, J., Yoo, K. Y., Beauchamp, J. L., Hodyss, R. P., Flagan, R. C., and Seinfeld, J. H.: Particle phase acidity and oligomer formation in secondary organic aerosol, *Environ. Sci. Technol.*, 38, 6582–6589, doi:10.1021/es049125k, 2004.
- Goldstein, A. H. and Galbally, I. E.: Known and unexplored organic constituents in the earth's atmosphere, *Environ. Sci. Technol.*, 41, 1514–1521, 2007.
- Guenther, A., Hewitt, C. N., Erickson, D., Fall, R., Geron, C., Graedel, T., Harley, P., Klinger, L., Lerdau, M., and McKay, W.: A global model of natural volatile organic compound emissions, *J. Geophys. Res.*, 100, 8873–8892, 1995.
- Guenther, A., Geron, C., Pierce, T., Lamb, B., Harley, P., and Fall, R.: Natural emissions of non-methane volatile organic compounds, carbon monoxide, and oxides of nitrogen from North America, *Atmos. Environ.*, 34, 2205–2230, 2000.
- Hallquist, M., Wenger, J. C., Baltensperger, U., Rudich, Y., Simpson, D., Claeys, M., Dommen, J., Donahue, N. M., George, C., Goldstein, A. H., Hamilton, J. F., Herrmann, H., Hoffmann, T., Iinuma, Y., Jang, M., Jenkin, M. E., Jimenez, J. L., Kiendler-Scharr, A., Maenhaut, W., McFiggans, G., Mentel, Th. F., Monod, A., Prévôt, A. S. H., Seinfeld, J. H., Surratt, J. D., Szmigielski, R., and Wildt, J.: The formation, properties and impact of secondary organic aerosol: current and emerging issues, *Atmos. Chem. Phys.*, 9, 5155–5236, doi:10.5194/acp-9-5155-2009, 2009.
- Hayen, H., Jachmann, N., Vogel, M., and Karst, U.: LC-electron capture APCI-MS for the determination of nitroaromatic compounds, *Analyst*, 127, 1027–1030, 2002.
- Heald, C., Kroll, J., Jimenez, J., Docherty, K., DeCarlo, P., Aiken, A., Chen, Q., Martin, S., Farmer, D., and Artaxo, P.: A simplified description of the evolution of organic aerosol com-

**SOA formation and composition from the photo-oxidation of methyl chavicol**

K. L. Pereira et al.

[Title Page](#)[Abstract](#)[Introduction](#)[Conclusions](#)[References](#)[Tables](#)[Figures](#)[◀](#)[▶](#)[◀](#)[▶](#)[Back](#)[Close](#)[Full Screen / Esc](#)[Printer-friendly Version](#)[Interactive Discussion](#)

position in the atmosphere, *Geophys. Res. Lett.*, 37, L08803, doi:10.1029/2010gl042737, 2010.

Healy, R. M., Temime, B., Kuprovskite, K., and Wenger, J. C.: Effect of relative humidity on gas/particle partitioning and aerosol mass yield in the photooxidation of *p*-xylene, *Environ. Sci. Technol.*, 43, 1884–1889, 2009.

Holčapek, M., Lísa, M., Volná, K., Almonasy, N., and Příklad, J.: Occurrence of radical molecular ions in atmospheric pressure chemical ionization mass spectra of heterocyclic compounds, *J. Mass Spectrom.*, 42, 1645–1648, doi:10.1002/jms.1318, 2007.

Holčapek, M., Jirásko, R., and Lísa, M.: Basic rules for the interpretation of atmospheric pressure ionization mass spectra of small molecules, *J. Chromatogr. A*, 1217, 3908–3921, 2010.

Holzinger, R., Lee, A., Paw, K. T., and Goldstein, U. A. H.: Observations of oxidation products above a forest imply biogenic emissions of very reactive compounds, *Atmos. Chem. Phys.*, 5, 67–75, doi:10.5194/acp-5-67-2005, 2005.

Holzinger, R., Kasper-Giebl, A., Staudinger, M., Schauer, G., and Röckmann, T.: Analysis of the chemical composition of organic aerosol at the Mt. Sonnblick observatory using a novel high mass resolution thermal-desorption proton-transfer-reaction mass-spectrometer (hr-TD-PTR-MS), *Atmos. Chem. Phys.*, 10, 10111–10128, doi:10.5194/acp-10-10111-2010, 2010.

Howard, J. A. and Ingold, K. U.: Self-reaction of sec-butylperoxy radicals. Confirmation of the Russell mechanism, *J. Am. Chem. Soc.*, 90, 1056–1058, doi:10.1021/ja01006a037, 1968.

Iinuma, Y., Böge, O., Keywood, M., Gnauk, T., and Herrmann, H.: Diaterpene acid acetate and diaterpenylic acid acetate: atmospheric tracers for secondary organic aerosol formation from 1,8-cineole oxidation, *Environ. Sci. Technol.*, 43, 280–285, doi:10.1021/es802141v, 2008.

Jang, M., Czochke, N. M., Lee, S., and Kamens, R. M.: Heterogeneous atmospheric aerosol production by acid-catalyzed particle-phase reactions, *Science*, 298, 814–817, 2002.

Jimenez, J. L., Canagaratna, M. R., Donahue, N. M., Prevot, A. S. H., Zhang, Q., Kroll, J. H., DeCarlo, P. F., Allan, J. D., Coe, H., Ng, N. L., Aiken, A. C., Docherty, K. S., Ulbrich, I. M., Grieshop, A. P., Robinson, A. L., Duplissy, J., Smith, J. D., Wilson, K. R., Lanz, V. A., Hueglin, C., Sun, Y. L., Tian, J., Laaksonen, A., Raatikainen, T., Rautiainen, J., Vaattovaara, P., Ehn, M., Kulmala, M., Tomlinson, J. M., Collins, D. R., Cubison, M. J., E., Dunlea, J., Huffman, J. A., Onasch, T. B., Alfarra, M. R., Williams, P. I., Bower, K., Kondo, Y., Schneider, J., Drewnick, F., Borrmann, S., Weimer, S., Demerjian, K., Salcedo, D., Cottrell, L., Griffin, R., Takami, A., Miyoshi, T., Hatakeyama, S., Shimono, A., Sun, J. Y.,

**SOA formation and composition from the photo-oxidation of methyl chavicol**

K. L. Pereira et al.

Title Page

Abstract

Introduction

Conclusions

References

Tables

Figures

◀

▶

◀

▶

Back

Close

Full Screen / Esc

Printer-friendly Version

Interactive Discussion

Zhang, Y. M., Dzepina, K., Kimmel, J. R., Sueper, D., Jayne, J. T., Herndon, S. C., Trimborn, A. M., Williams, L. R., Wood, E. C., Middlebrook, A. M., Kolb, C. E., Baltensperger, U., and Worsnop, D. R.: Evolution of organic aerosols in the atmosphere, *Science*, 326, 1525–1529, doi:10.1126/science.1180353, 2009.

5 Kind, T. and Fiehn, O.: Metabolomic database annotations via query of elemental compositions: mass accuracy is insufficient even at less than 1 ppm, *BMC Bioinformatics*, 7, 234, doi:10.1186/1471-2105-7-234, 2006.

Klotz, B., Sørensen, S., Barnes, I., Becker, K. H., Etzkorn, T., Volkamer, R., Platt, U., Wirtz, K., and Martín-Reviejo, M.: Atmospheric oxidation of toluene in a large-volume outdoor photoreactor: in situ determination of ring-retaining product yields, *J. Phys. Chem. A*, 102, 10289–10299, 1998.

10 Kroll, J. H. and Seinfeld, J. H.: Chemistry of secondary organic aerosol: formation and evolution of low-volatility organics in the atmosphere, *Atmos. Environ.*, 42, 3593–3624, doi:10.1016/j.atmosenv.2008.01.003, 2008.

15 Lee, A., Goldstein, A. H., Keywood, M. D., Gao, S., Varutbangkul, V., Bahreini, R., Ng, N. L., Flagan, R. C., and Seinfeld, J. H.: Gas-phase products and secondary aerosol yields from the ozonolysis of ten different terpenes, *J. Geophys. Res.*, 111, D07302, doi:10.1029/2005JD006437, 2006a.

20 Lee, A., Goldstein, A. H., Kroll, J. H., Ng, N. L., Varutbangkul, V., Flagan, R. C., and Seinfeld, J. H.: Gas-phase products and secondary aerosol yields from the photooxidation of 16 different terpenes, *J. Geophys. Res.*, 111, D17305, doi:10.1029/2006JD007050, 2006b.

Madronich, S. and Calvert, J. G.: Permutation reactions of organic peroxy radicals in the troposphere, *J. Geophys. Res.-Atmos.*, 95, 5697–5715, doi:10.1029/JD095iD05p05697, 1990.

25 March, J.: *Advanced Organic Chemistry: Reactions, Mechanisms, and Structure*, John Wiley & Sons, New York, 1992.

Mirov, N. T.: *Composition of Gum Turpentine of Pines*, USDA forest service, Technical Bulletin No. 1239, 158 pp., 1961.

Misztal, P. K., Owen, S. M., Guenther, A. B., Rasmussen, R., Geron, C., Harley, P., Phillips, G. J., Ryan, A., Edwards, D. P., Hewitt, C. N., Nemitz, E., Siong, J., Heal, M. R., and Cape, J. N.: Large estragole fluxes from oil palms in Borneo, *Atmos. Chem. Phys.*, 10, 4343–4358, doi:10.5194/acp-10-4343-2010, 2010.

30 Nannoolal, Y., Rarey, J., Ramjugernath, D., and Cordes, W.: Estimation of pure component properties: Part 1. Estimation of the normal boiling point of non-electrolyte organic com-

**SOA formation and composition from the photo-oxidation of methyl chavicol**

K. L. Pereira et al.

Title Page

Abstract

Introduction

Conclusions

References

Tables

Figures

⏪

⏩

◀

▶

Back

Close

Full Screen / Esc

Printer-friendly Version

Interactive Discussion

pounds via group contributions and group interactions, *Fluid Phase Equilibr.*, 226, 45–63, doi:10.1016/j.fluid.2004.09.001, 2004.

Nannoolal, Y., Rarey, J., and Ramjugernath, D.: Estimation of pure component properties: Part 3. Estimation of the vapor pressure of non-electrolyte organic compounds via group contributions and group interactions, *Fluid Phase Equilibria*, 269, 117–133, 2008.

Neeb, P., Horie, O., and Moortgat, G. K.: Gas-phase ozonolysis of ethene in the presence of hydroxylic compounds, *Int. J. Chem. Kinet.*, 28, 721–730, doi:10.1002/(sici)1097-4601(1996)28:10<721::aid-kin2>3.0.co;2-p, 1996.

Official Portal of Malaysian Palm Oil Board: available at: <http://bepi.mpob.gov.my/> (last access: 11 April 2013), 2012.

Odum, J. R., Hoffmann, T., Bowman, F., Collins, D., Flagan, R. C., and Seinfeld, J. H.: Gas/particle partitioning and secondary organic aerosol yields, *Environ. Sci. Technol.*, 30, 2580–2585, doi:10.1021/es950943+, 1996.

Orlando, J. J., Tyndall, G. S., and Wallington, T. J.: The atmospheric chemistry of alkoxy radicals, *Chem. Rev.*, 103, 4657–4690, 2003.

Orzechowska, G. E. and Paulson, S. E.: Photochemical sources of organic acids. 1. Reaction of ozone with isoprene, propene, and 2-butenes under dry and humid conditions using SPME, *J. Phys. Chem. A*, 109, 5358–5365, doi:10.1021/jp050166s, 2005.

O’Neal, H. E. and Blumstein, C.: A new mechanism for gas phase ozone–olefin reactions, *Int. J. Chem. Kinet.*, 5, 397–413, 1973.

Peeters, J., Boullart, W., Pultau, V., Vandenberg, S., and Vereecken, L.: Structure-activity relationship for the addition of OH to (poly)alkenes: site-specific and total rate constants, *J. Phys. Chem. A*, 111, 1618–1631, doi:10.1021/jp066973o, 2007.

Pellegrin, V.: Molecular formulas of organic compounds: the nitrogen rule and degree of unsaturation, *J. Chem. Educ.*, 60, p. 626, doi:10.1021/ed060p626, 1983.

Pöschl, U.: Atmospheric aerosols: composition, transformation, climate and health effects, *Angew. Chem. Int. Edit.*, 44, 7520–7540, doi:10.1002/anie.200501122, 2005.

Rickard, A. R., Wyche, K. P., Metzger, A., Monks, P. S., Ellis, A. M., Dommen, J., Baltensperger, U., Jenkin, M. E., and Pilling, M. J.: Gas phase precursors to anthropogenic secondary organic aerosol: using the master chemical mechanism to probe detailed observations of 1,3,5-trimethylbenzene photo-oxidation, *Atmos. Environ.*, 44, 5423–5433, doi:10.1016/j.atmosenv.2009.09.043, 2010.

**SOA formation and composition from the photo-oxidation of methyl chavicol**

K. L. Pereira et al.

[Title Page](#)[Abstract](#)[Introduction](#)[Conclusions](#)[References](#)[Tables](#)[Figures](#)[⏪](#)[⏩](#)[◀](#)[▶](#)[Back](#)[Close](#)[Full Screen / Esc](#)[Printer-friendly Version](#)[Interactive Discussion](#)

- Schade, G. W. and Goldstein, A. H.: Fluxes of oxygenated volatile organic compounds from a ponderosa pine plantation, *J. Geophys. Res.*, 106, 3111–3123, 2001.
- Schmidt, A.-C., Herzsich, R., Matysik, F.-M., and Engewald, W.: Investigation of the ionisation and fragmentation behaviour of different nitroaromatic compounds occurring as polar metabolites of explosives using electrospray ionisation tandem mass spectrometry, *Rapid Commun. Mass Sp.*, 20, 2293–2302, doi:10.1002/rcm.2591, 2006.
- Singh, H., Chen, Y., Tabazadeh, A., Fukui, Y., Bey, I., Yantosca, R., Jacob, D., Arnold, F., Wohlfahrt, K., Atlas, E., Flocke, F., Blake, D., Blake, N., Heikes, B., Snow, J., Talbot, R., Gregory, G., Sachse, G., Vay, S., and Kondo, Y.: Distribution and fate of selected oxygenated organic species in the troposphere and lower stratosphere over the Atlantic, *J. Geophys. Res.-Atmos.*, 105, 3795–3805, doi:10.1029/1999jd900779, 2000.
- Solomon, S., Qin, D., Manning, M., Chen, Z., Marquis, M., Averyt, K., Tignor, M., and Miller, H.: *Climate change 2007: the physical science basis: working Group I contribution to the fourth assessment report of the IPCC*, Cambridge University Press, Cambridge, 2007.
- Song, C., Na, K., and Cocker, D. R.: Impact of the hydrocarbon to NO<sub>x</sub> ratio on secondary organic aerosol formation, *Environ. Sci. Technol.*, 39, 3143–3149, doi:10.1021/es0493244, 2005.
- Southwell, I. A., Russell, M. F., Smith, R. L., and Vinnicombe, A.: *Ochrosperma lineare*, a new source of methyl chavicol, *J. Essent. Oil Res.*, 15, 329–330, 2003.
- Spada, N., Fujii, E., and Cahill, T. M.: Diurnal cycles of acrolein and other small aldehydes in regions impacted by vehicle emissions, *Environ. Sci. Technol.*, 42, 7084–7090, doi:10.1021/es801656e, 2008.
- Steiner, A. L., Cohen, R. C., Harley, R. A., Tonse, S., Millet, D. B., Schade, G. W., and Goldstein, A. H.: VOC reactivity in central California: comparing an air quality model to ground-based measurements, *Atmos. Chem. Phys.*, 8, 351–368, doi:10.5194/acp-8-351-2008, 2008.
- Stockwell, W. R., Middleton, P., Chang, J. S., and Tang, X.: The second generation regional acid deposition model chemical mechanism for regional air quality modeling, *J. Geophys. Res.*, 95, 16343–16367, 1990.
- Taipale, R., Rantala, P., Kajos, M., Patokoski, J., Ruuskanen, T., Aalto, J., Kolari, P., Bäck, J., Hari, P., Kulmala, M., and Rinne, J.: Oxygenated VOC and monoterpene emissions from a boreal coniferous forest, *EGU General Assembly Conference Abstracts*, 9735, 2012.

United States Department of Agriculture, Global Crop Production Analysis: available at: <http://www.pecad.fas.usda.gov> (last access: 11 April 2013), 2013.

Varutbangkul, V., Brechtel, F. J., Bahreini, R., Ng, N. L., Keywood, M. D., Kroll, J. H., Flanagan, R. C., Seinfeld, J. H., Lee, A., and Goldstein, A. H.: Hygroscopicity of secondary organic aerosols formed by oxidation of cycloalkenes, monoterpenes, sesquiterpenes, and related compounds, *Atmos. Chem. Phys.*, 6, 2367–2388, doi:10.5194/acp-6-2367-2006, 2006.

Werker, E., Putievsky, E., Ravid, U., Dudai, N., and Katzir, I.: Glandular Hairs, Secretory Cavities, and the Essential Oil in the Leaves of Tarragon (*Artemisia dracunculus* L.), *Journal of Herbs, Spices Med. Plants*, 2, 19–32, 1994.

Wiedinmyer, C., Guenther, A., Harley, P., Hewitt, N., Geron, C., Artaxo, P., Steinbrecher, R., and Rasmussen, R.: Global Organic Emissions from Vegetation, in: Emissions of Atmospheric Trace Compounds, edited by: Granier, C., Artaxo, P., and Reeves, C., *Advances in Global Change Research*, Springer Netherlands, 115–170, 2004.

Yinon, J., McClellan, J. E., and Yost, R. A.: Electrospray ionization tandem mass spectrometry collision-induced dissociation study of explosives in an ion trap mass spectrometer, *Rapid Commun. Mass Sp.*, 11, 1961–1970, doi:10.1002/(sici)1097-0231(199712)11:18<1961::aid-rcm99>3.0.co;2-k, 1997.

Zhao, X. and Yinon, J.: Identification of nitrate ester explosives by liquid chromatography–electrospray ionization and atmospheric pressure chemical ionization mass spectrometry, *J. Chromatogr. A*, 977, 59–68, doi:10.1016/S0021-9673(02)01349-3, 2002.

Zhou, Y., Zhang, H., Parikh, H. M., Chen, E. H., Rattanavaraha, W., Rosen, E. P., Wang, W., and Kamens, R. M.: Secondary organic aerosol formation from xylenes and mixtures of toluene and xylenes in an atmospheric urban hydrocarbon mixture: water and particle seed effects (II), *Atmos. Environ.*, 45, 3882–3890, doi:10.1016/j.atmosenv.2010.12.048, 2011.

Ziemann, P. J. and Atkinson, R.: Kinetics, products, and mechanisms of secondary organic aerosol formation, *Chem. Soc. Rev.*, 41, 6582–6605, doi:10.1039/c2cs35122f, 2012.

Zimmerman, P. R.: Testing of hydrocarbon emissions from vegetation, leaf litter and aquatic surfaces, and development of a methodology for compiling biogenic emission inventories, Final Report, Washington State University Pullman, Washington, 1979.

ACPD

13, 33105–33144, 2013

## SOA formation and composition from the photo-oxidation of methyl chavicol

K. L. Pereira et al.

Title Page

Abstract

Introduction

Conclusions

References

Tables

Figures

⏪

⏩

◀

▶

Back

Close

Full Screen / Esc

Printer-friendly Version

Interactive Discussion

## SOA formation and composition from the photo-oxidation of methyl chavicol

K. L. Pereira et al.

**Table 1.** The initial experimental mixing ratios, temperature and relative humidity range for the experiments discussed.

Exp.	Date	Exp. description	Initial mixing ratio <sup>a</sup>				Experimental range <sup>b</sup>	
			MC <sup>c</sup> [ppbv]	NO [ppbv]	NO <sub>2</sub> [ppbv]	O <sub>3</sub> [ppbv]	Temp [K]	RH [%]
MC <sub>(0)</sub>	8 May 2012	Chamber background	0	0.3	0.7	0	294–312	0.7–4.7
MC <sub>low</sub>	11 May 2012	Photosmog low concentration	212	38	8	2	298–308	0.9–14.7
MC <sub>high</sub>	15 May 2012	Photosmog high concentration	460	9	3	5	297–306	2.1–10.7

<sup>a</sup> On the opening of the chamber covers.

<sup>b</sup> From the opening to the closing of the chamber covers.

<sup>c</sup> FTIR measurement.

[Title Page](#)
[Abstract](#)
[Introduction](#)
[Conclusions](#)
[References](#)
[Tables](#)
[Figures](#)
[Back](#)
[Close](#)
[Full Screen / Esc](#)
[Printer-friendly Version](#)
[Interactive Discussion](#)

## SOA formation and composition from the photo-oxidation of methyl chavicol

K. L. Pereira et al.

Title Page

Abstract

Introduction

Conclusions

References

Tables

Figures

◀

▶

◀

▶

Back

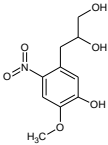
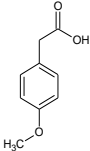
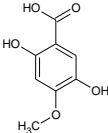
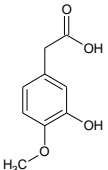
Close

Full Screen / Esc

Printer-friendly Version

Interactive Discussion

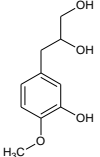
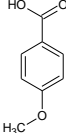
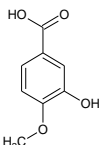
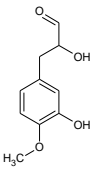
**Table 2.** The 10 structurally identified SOA compounds including; retention time ( $t_R$ ), molecular formula (MF) identification and associated errors using HPLC-ITMS, FTICR-MS and HPLC-QTOFMS.

Compound	IUPAC name	Compound structure	MC <sub>high</sub>					
			MW [g mol <sup>-1</sup> ]	$t_R$	FTICR-MS MF	FTICR-MS MF error [ppm]	HPLC-QTOFMS MF	HPLC-QTOFMS MF error [ppm]
1	3-(5-hydroxy-4-methoxy-2-nitrophenyl)propane-1,2-diol		243	22.2	C <sub>10</sub> H <sub>13</sub> NO <sub>6</sub>	0.6	C <sub>10</sub> H <sub>13</sub> NO <sub>6</sub>	-0.7
2	(4-methoxyphenyl)acetic acid		166	28.1	C <sub>9</sub> H <sub>10</sub> O <sub>3</sub>	0.8	C <sub>9</sub> H <sub>10</sub> O <sub>3</sub>	1.2
3	2,5-dihydroxy-4-methoxybenzoic acid		184	10.2	<sup>a</sup>		C <sub>9</sub> H <sub>8</sub> O <sub>5</sub>	48
4	(3-hydroxy-4-methoxyphenyl)acetic acid		182	16.1	C <sub>9</sub> H <sub>10</sub> O <sub>4</sub>	0.8	C <sub>9</sub> H <sub>10</sub> O <sub>4</sub>	-0.3

## SOA formation and composition from the photo-oxidation of methyl chavicol

K. L. Pereira et al.

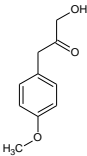
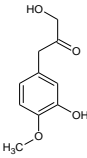
Table 2. Continued.

Compound	IUPAC name	Compound structure	MC <sub>high</sub>					
			MW [g mol <sup>-1</sup> ]	t <sub>R</sub>	FTICR-MS MF	FTICR-MS MF error [ppm]	HPLC-QTOFMS MF	HPLC-QTOFMS MF error [ppm]
5	3-(3-hydroxy-4-methoxyphenyl)propane-1,2-diol		198	20.2	C <sub>10</sub> H <sub>14</sub> O <sub>4</sub>	0.9	C <sub>10</sub> H <sub>14</sub> O <sub>4</sub>	2.4
6	4-methoxybenzoic acid		152	30.1	C <sub>8</sub> H <sub>8</sub> O <sub>3</sub>	0.3	C <sub>8</sub> H <sub>8</sub> O <sub>3</sub>	-1.4
7	3-hydroxy-4-methoxybenzoic acid		168	33.0	C <sub>8</sub> H <sub>8</sub> O <sub>4</sub>	1.2	C <sub>8</sub> H <sub>8</sub> O <sub>4</sub>	0.2
8	2-hydroxy-3-(3-hydroxy-4-methoxyphenyl)propanal		196	25.2	C <sub>10</sub> H <sub>12</sub> O <sub>4</sub>	1	C <sub>10</sub> H <sub>12</sub> O <sub>4</sub>	2.5

## SOA formation and composition from the photo-oxidation of methyl chavicol

K. L. Pereira et al.

Table 2. Continued.

Compound	IUPAC name	Compound structure	MC <sub>high</sub>					
			MW [g mol <sup>-1</sup> ]	t <sub>R</sub>	FTICR-MS MF	FTICR-MS MF error [ppm]	HPLC-QTOFMS MF	HPLC-QTOFMS MF error [ppm]
9	1-hydroxy-3-(4-methoxyphenyl)propan-2-one		180	27.6	<sup>a</sup>		C <sub>10</sub> H <sub>12</sub> O <sub>3</sub>	-7.8
10	1-hydroxy-3-(3-hydroxy-4-methoxyphenyl)propan-2-one		196	19.8	C <sub>10</sub> H <sub>12</sub> O <sub>4</sub> <sup>b</sup>	5	C <sub>10</sub> H <sub>12</sub> O <sub>4</sub> <sup>b</sup>	9.4

<sup>a</sup> Deprotonated or protonated molecular species not observed in FTICR-MS spectra due to low concentration.<sup>b</sup> Identified as [M + Na]<sup>+</sup>, the Na adduct has been removed from molecular formula and molecular weight corrected.

## SOA formation and composition from the photo-oxidation of methyl chavicol

K. L. Pereira et al.

**Table 3.** Deprotonated molecular species fragmentation for compound 1, obtained from the use of the HPLC-ITMS<sup>2</sup> and the HPLC-QTOFMS<sup>2</sup>.

MF	[M–H] <sup>–</sup>	DBE	Fragment ion [m/z]	Fragment ion MF	DBE	Loss [Da]	Electron fragmentation	Fragment ion MF error [ppm]	MF Score [%]	Fragmentation shown
C <sub>10</sub> H <sub>13</sub> NO <sub>6</sub>	242	5	<b>224</b>	<b>C<sub>10</sub>H<sub>10</sub>NO<sub>5</sub></b>	<b>6</b>	<b>18</b>	<b>EE</b>	<b>–2.1</b>	<b>100</b>	<b>Fig. 2a</b>
			182	C <sub>8</sub> H <sub>8</sub> NO <sub>4</sub>	5	(18 + 42) = 60	EE	–1	100	Fig. 2b
			167	C <sub>7</sub> H <sub>5</sub> NO <sub>4</sub>	5 <sup>a</sup>	(18 + 57) = 75	OE	8.8	100	Fig. 2c
			137	C <sub>7</sub> H <sub>5</sub> O <sub>3</sub>	4 <sup>b</sup>	105	OE	–19.2	100	Fig. 2c

The highest intensity fragment ion is shown in bold. DBE = double bond equivalent. Electron fragmentation, EE = even electron, OE = odd electron. MF = molecular formula.

<sup>a</sup> DBE was manually calculated, as automated DBE calculation is incorrect for radical fragment ions (DBE = 5.5–0.5 (for one “hydrogen atom deficiency”) = 5, see Pellegrin (1983) for the calculation of DBE and DBE correction for radical ions).

<sup>b</sup> DBE manually calculated, (DBE = 5–1 (for two “hydrogen atom deficiencies”) = 4).

Title Page

Abstract

Introduction

Conclusions

References

Tables

Figures

⏪

⏩

◀

▶

Back

Close

Full Screen / Esc

Printer-friendly Version

Interactive Discussion

## SOA formation and composition from the photo-oxidation of methyl chavicol

K. L. Pereira et al.

**Table 4.** Deprotonated molecular species fragmentation for compound 5, obtained from the use of the HPLC-ITMS<sup>2</sup> and the HPLC-QTOFMS<sup>2</sup>.

MF	[M–H] <sup>–</sup>	DBE	Fragment ion [m/z]	Fragment ion MF	DBE	Loss [Da]	Electron fragmentation	Fragment ion MF error [ppm]	MF Score [%]	Fragmentation shown
C <sub>10</sub> H <sub>14</sub> O <sub>4</sub>	197	4	<b>179</b>	<b>C<sub>10</sub>H<sub>11</sub>O<sub>3</sub></b>	<b>5</b>	<b>18</b>	<b>EE</b>	<b>–19.3</b>	<b>100</b>	<b>Fig. 3a</b>
			137	C <sub>8</sub> H <sub>9</sub> O <sub>2</sub>	4	(18 + 42) = 60	EE	–0.5	100	Fig. 3b
			123	C <sub>7</sub> H <sub>7</sub> O <sub>2</sub>	4	74	EE	–3.4	100	Fig. 3c

The highest intensity fragment ion is shown in bold. DBE = double bond equivalent. Electron fragmentation, EE = even electron. MF = molecular formula.

Title Page

Abstract

Introduction

Conclusions

References

Tables

Figures

◀

▶

◀

▶

Back

Close

Full Screen / Esc

Printer-friendly Version

Interactive Discussion

## SOA formation and composition from the photo-oxidation of methyl chavicol

K. L. Pereira et al.

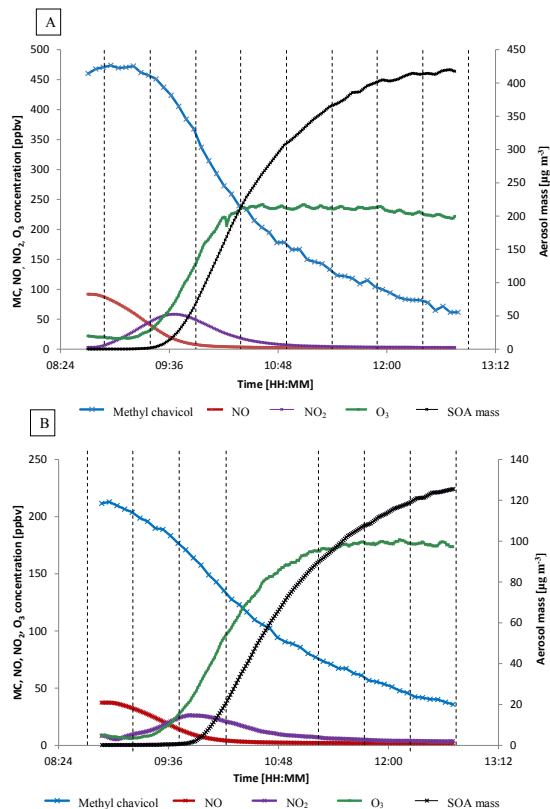


**Fig. 1.** Temporal profiles of methyl chavicol, O<sub>3</sub>, NO, NO<sub>2</sub> and SOA mass for MC<sub>low</sub> and MC<sub>high</sub> from the opening to the closing of the chamber housing. **(A)** MC<sub>high</sub>, (opening chamber housing = 8.42 a.m., closing of chamber housing 12.45 p.m.) **(B)** = MC<sub>low</sub>, (opening chamber housing = 8.52 a.m., closing of chamber housing 12.42 p.m.). SOA mass is displayed on the secondary y-axis and corrected for wall loss and chamber dilution. Dashed lines display the PILS sample start time. PILS sample start time 10.43 a.m. in MC<sub>low</sub> broken during transport.

## SOA formation and composition from the photo-oxidation of methyl chavicol

K. L. Pereira et al.

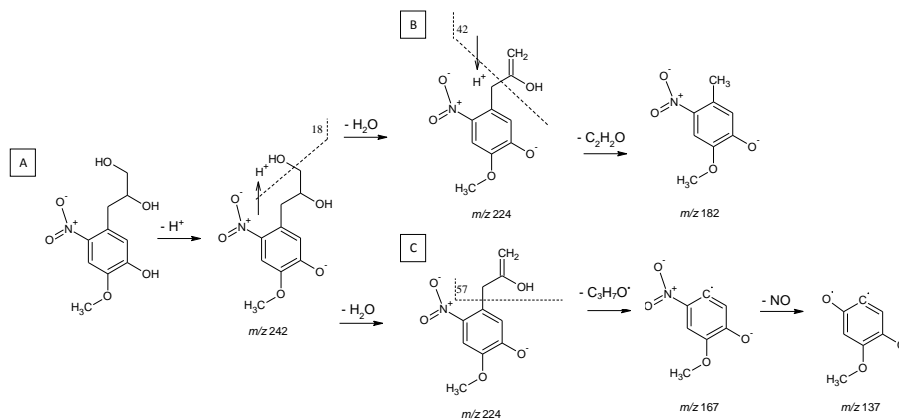


**Fig. 2.** Proposed deprotonated molecular species fragmentation for compound 1 in negative ionisation mode. Dashed lines indicate the location of fragmentation.

## SOA formation and composition from the photo-oxidation of methyl chavicol

K. L. Pereira et al.

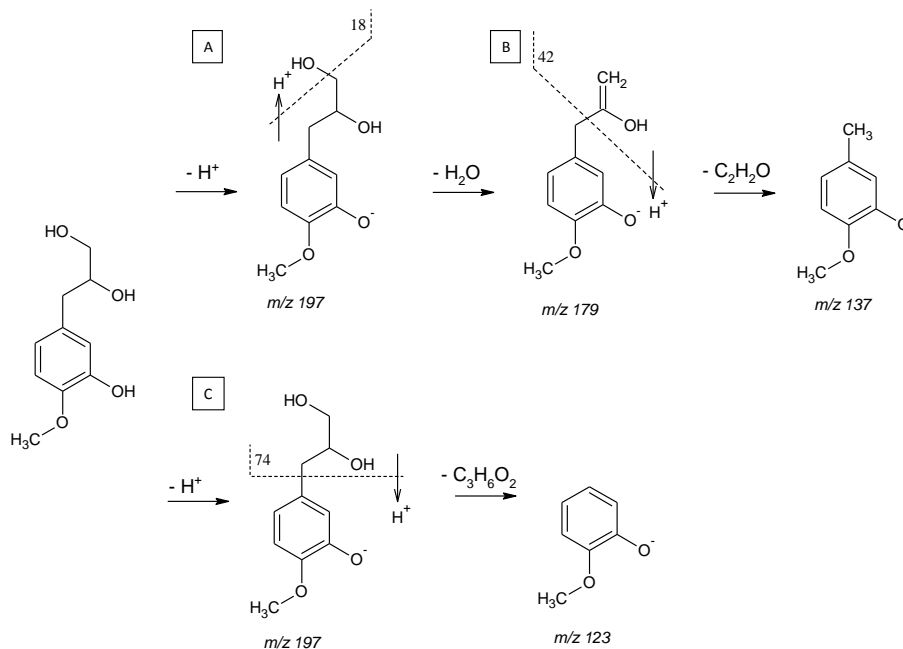


**Fig. 3.** Proposed deprotonated molecular species fragmentation for compound 5 in negative ionisation mode. Dashed lines indicate the location of fragmentation.

## SOA formation and composition from the photo-oxidation of methyl chavicol

K. L. Pereira et al.

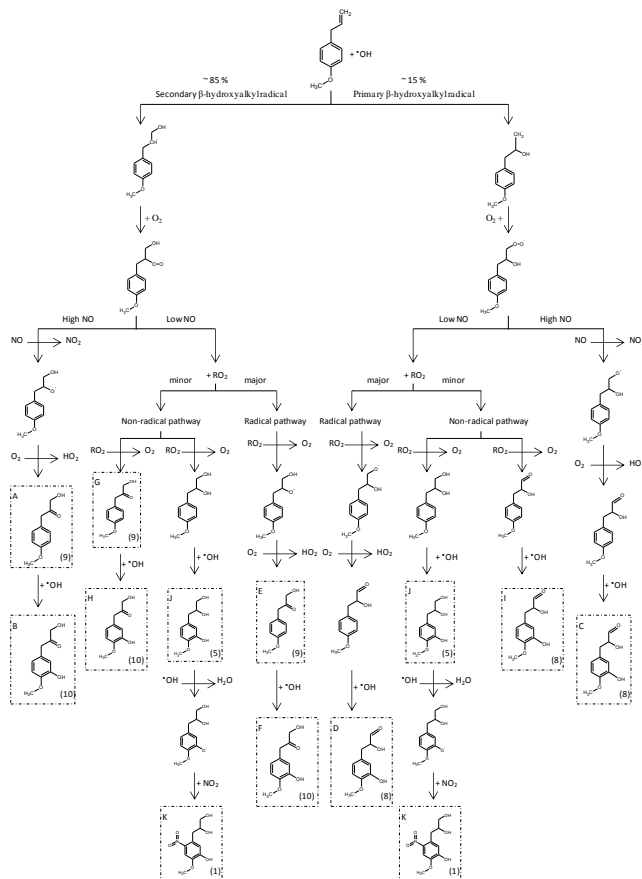


**Fig. 4.** Mechanism of formation for the identified SOA compounds, compounds 1, 5, 8, 9 and 10, shown in brackets, refer to Table 2 for compound identification. See text for the explanation of the mechanism, letters refer to the text explanation. Boxes highlight identified SOA compounds.

Title Page

Abstract

Introduction

Conclusions

References

Tables

Figures

◀

▶

◀

▶

Back

Close

Full Screen / Esc

Printer-friendly Version

Interactive Discussion

## SOA formation and composition from the photo-oxidation of methyl chavicol

K. L. Pereira et al.

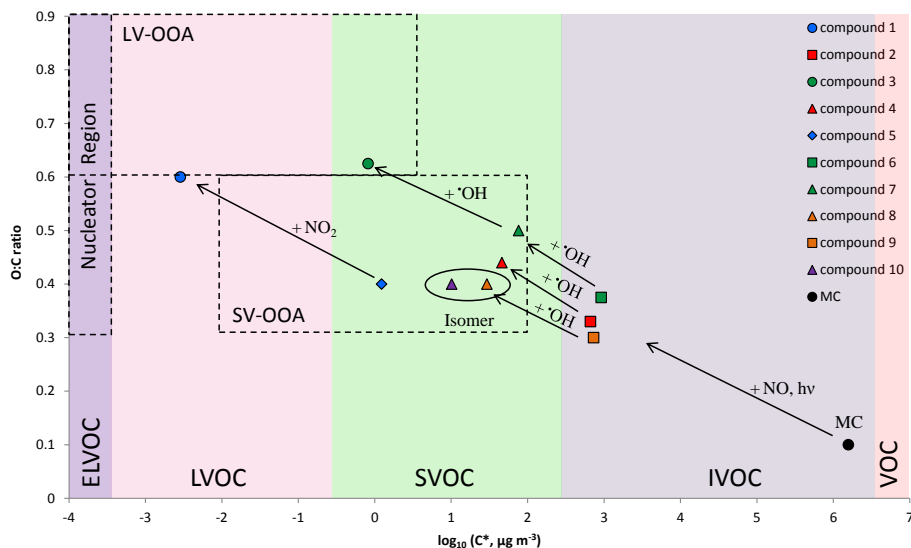


**Fig. 5.** Oxygen to carbon ratio (O : C) and saturation concentration  $\log_{10}(C^*, \mu\text{g m}^{-3})$  (Donahue et al., 2006b) space to show the movement of the identified SOA compounds to lower volatilities upon oxidation in  $\text{MC}_{\text{high}}$ . Related generations of compounds are shown in the same colour. The change of shape but use of the same colour indicates a change in the SOA compound structure through the reaction with  $\cdot\text{OH}$  radicals or  $\text{NO}_2$ . See legend for SOA compound identification and refer to Table 2. O : C/ $\log_{10}(C^*, \mu\text{g m}^{-3})$  space with associated volatilities have been redrawn from Donahue et al. (2013) and Jimenez et al. (2009).

Title Page

Abstract

Introduction

Conclusions

References

Tables

Figures

◀

▶

◀

▶

Back

Close

Full Screen / Esc

Printer-friendly Version

Interactive Discussion